THE ASTROPHYSICAL JOURNAL, 559:53–58, 2001 September 20

DETERMINING THE FRACTION OF COMPACT OBJECTS IN THE UNIVERSE USING SUPERNOVA OBSERVATIONS

E. MÖRTSELL,[1] A. GOOBAR,[1] AND L. BERGSTRÖM[1]
Received 2001 April 3; accepted 2001 May 24

ABSTRACT

We investigate the possibility of determining the fraction of compact objects in the universe by studying gravitational lensing effects on Type Ia supernova observations. Using simulated data sets from 1 yr of operation of the proposed dedicated supernova detection satellite *Supernova/Acceleration Probe*, we find that it should be possible to determine the fraction of compact objects to an accuracy of $\lesssim 5\%$.

Subject headings: dark matter — gravitational lensing — supernovae: general

1. INTRODUCTION

Recent measurements of anisotropies in the cosmic microwave background radiation (CMBR) show that the universe is very close to flat, i.e., $\Omega_{\rm tot} \approx 1$ (Netterfield et al. 2001; Stompor et al. 2001; Pryke et al. 2001). Since observations of Type Ia supernovae (SNe Ia) indicate that the expansion rate of the universe is accelerating, the major part of this total energy should have negative pressure, e.g., in the form of the cosmological constant corresponding to $\Omega_\Lambda \sim 0.7$ in a flat universe (Perlmutter et al. 1999; Riess et al. 1998), in agreement with constraints on the matter density Ω_M from cluster abundances (Bahcall & Fan 1998; Carlberg et al. 1999) and large-scale structure (Peacock et al. 2001). Thus, a concordance model with $\Omega_M \approx 0.3$ and $\Omega_\Lambda \approx 0.7$ has emerged.

The constitution of the total matter density is a matter of intense theoretical and experimental research. The energy density in baryonic matter as derived from big bang nucleosynthesis (BBN) is given by $\Omega_b h^2 = 0.019 \pm 0.0024$ (Burles et al. 1999), whereas CMBR measurements yield $\Omega_b h^2 = 0.02^{+0.06}_{-0.01}$ (Wang, Tegmark, & Zaldarriaga 2001). Either way, the matter density in baryons is almost an order of magnitude smaller than the nonbaryonic dark matter (DM) component. However, the BBN range for the baryon density still means that most of the baryonic matter is also dark (see, e.g., Persic & Salucci 1992 and references therein).

There are various possible places for the dark baryons to hide; examples are warm gas in groups and clusters, which is difficult to detect at present (Fukugita, Hogan, & Peebles 1998), or in the form of massive compact halo objects (MACHOs), where indeed there have been detections (Alcock et al. 2000; Lasserre et al. 2000). The long lines of sight to distant supernovae means that they are well suited to probe the matter content along the paths of the light rays, where gravitational lensing may occur where there are matter accumulations. Compact objects give more distinct lensing effects, enabling a distinction between diffuse matter and compact bodies along the light path. In particular, it may be possible to investigate whether the halo fraction deduced for the Milky Way from microlensing along the line of sight to the Large Magellanic Cloud, on the order of 20% (Alcock et al. 2000), is a universal number or if the average cosmological fraction is larger or smaller.

Regardless of its constitution, we can classify DM according to its clustering properties. In this paper we will use the terminology of *smooth DM* for DM candidates that tend to be smooth on subgalaxy scales, e.g., weakly interacting massive particles (WIMPs) such as neutralinos. The term *compact DM* will be reserved for MACHOs such as brown or white dwarfs and primordial black holes (Jedamzik 1998).

An advantage with gravitational lensing is that its effects can determine the distribution of DM independent of its constitution or its dynamical state. The topic of this paper concerns the use of the gravitational magnification of standard candles, such as SNe Ia, to determine the fraction of compact objects in a cosmological context.

In an early study, Rauch (1991) concluded that with a sample of 1000 SNe Ia at redshift $z \approx 1$, one should be able to discriminate between the extreme cases of all DM as smooth or as compact objects. More recent work (Metcalf & Silk 1999; Goliath & Mörtsell 2000) has shown that a sample of 50–100 SNe should be sufficient to make the same discrimination. Seljak & Holz (1999) have found that it should be possible to actually determine the fraction of compact objects to 20% accuracy with 100–400 SNe Ia at $z = 1$. In this work we extend these studies by exploring the possibility of determining the fraction of compact objects using a future sample of SNe Ia distributed over a broad redshift range, with the intrinsic spread of absolute luminosity of the SNe and expected measurement error for a proposed space-borne mission, *Supernova/Acceleration Probe* (*SNAP*),[2] taken into account.

In § 2 we clarify the distinction between compact and noncompact DM objects. In § 3 we discuss gravitational lensing of SNe, and in § 4, we present the Monte Carlo simulation package used to predict this effect. Section 5 is concerned with the proposed satellite telescope that will be able to produce the data sets used in this study; in § 6 we present our results. The paper is concluded with a summary in § 7.

2. COMPACT OBJECTS

For an object to be compact in a lensing context, we demand that it be contained within its own Einstein radius, $r_{\rm E}$. For a DM clump at $z = 0.5$ and a source at $z = 1$, $r_{\rm E} \sim 10^{-2}(M/M_\odot)^{1/2}$ pc in a $\Omega_M = 0.3$, $\Omega_\Lambda = 0.7$, and $h = 0.65$ cosmology. Also, the Einstein radius projected on the source plane should be larger than the size of the source. An SN Ia at maximum luminosity has a size of $\sim 10^{15}$ cm,

[1] Department of Physics, Stockholm University, S-106 91 Stockholm, Sweden; edvard@physto.se, ariel@physto.se, lbe@physto.se.

[2] The *SNAP* Science Proposal 2000 is available at http://snap.lbl.gov.

implying a lower mass limit of $\sim 10^{-4}\ M_\odot$ for the case described above.

The effects of lensing by compact objects are different from those of lensing by halos consisting of smoothly distributed DM, such as in the singular isothermal sphere or Navarro-Frenk-White (NFW) density profile (Navarro, Frenk, & White 1997), one of the differences being the tail of large magnifications caused by small impact-parameter lines of sight near the compact objects. However, N-body simulations also predict, besides the overall cuspy profiles of ordinary Galaxy-sized DM halos, a large number of small subhalos on all length scales that can been resolved (Navarro et al. 1997; Ghigna et al. 2000). The number density of the smaller objects, of mass M, follows approximately the law $dN/dM \propto M^{-2}$, as predicted by Press-Schechter theory. Thus, one may expect a multitude of subhalos in each galaxy or cluster halo. In addition, N-body simulations show the less massive halos to be denser (mainly owing to their being formed early when the background density was higher). Thus, it is appropriate to address the question pf whether this type of small-scale structure, and in particular the dense central regions of them, may give rise to lensing effects similar to the ones caused by truly compact objects.

To put a bound on these possible effects, we use the results of the most accurate numerical simulations to date (Ghigna et al. 2000). The density profiles within DM clumps obtained in the simulations can be fitted by the Moore profile

$$\rho_M(r) = \frac{\rho'_M}{(r/a)^{1.5}[1 + (r/a)^{1.5}]} . \quad (1)$$

Here ρ'_M and a are not independent parameters but related by the concentration parameter $c_M = R_{200}/a$, which depends on mass roughly as

$$c_M \sim 10.6 M_{12}^{-0.084} . \quad (2)$$

(Here M_{12} is the virial mass in units of $10^{12}\ M_\odot$; R_{200} is the virial radius where the average overdensity is 200 times the background density. Similar relations appear in the NFW simulations.)

Using these relations we can derive the mass M_R (also in units of $10^{12}\ M_\odot$) within distance $R_{\rm pc}$ parsecs from the center of the halo,

$$M_R \sim 10^{-7} M_{12}^{0.4} R_{\rm pc}^{1.5} . \quad (3)$$

Comparing this with the Einstein radius for the same mass for a lensing event of typical distance gigaparsecs, $D_{\rm Gpc}$,

$$R_{\rm E} \sim 10^4 M_R^{0.5} D_{\rm Gpc}^{0.5}\ {\rm pc} , \quad (4)$$

we find that M_R is within its own Einstein radius if

$$M_R \lesssim 10^{-4} M_{12}^{1.6} D_{\rm Gpc}^3 . \quad (5)$$

The requirement that the lensing mass is greater than $10^{-4}\ M_\odot$ means that DM clumps of the Moore type with mass greater than around $10^4\ M_\odot$ ($M_{12} > 10^{-8}$) will, in principle, contribute to compact lensing. However, it is only the very central, dense core that can contribute to the lensing, and we see from equation (5) that only a small fraction f of the mass in the clump is within its own Einstein radius,

$$f = \frac{M_R}{M_{12}} \sim 10^{-4} M_{12}^{0.6} D_{\rm Gpc}^3 . \quad (6)$$

Thus, only clumps of Galaxy size contribute appreciably to the lensing, and this part is included in our standard calculations.

Since this analysis was made for Moore-type halos, which are more concentrated than NFW halos, we conclude that compact objects detected through lensing of supernovae cannot, according to current thinking about structure formation, be caused by clumps of particle DM formed through hierarchical clustering.

3. GRAVITATIONAL LENSING OF SUPERNOVAE

The effect of gravitational lensing on SN Ia measurements is to cause a dispersion in the Hubble diagram. In Figure 1 we compare the dispersion owing to gravitational lensing with the intrinsic dispersion and the typical measurement error for SNe Ia. In the upper left panel, we show an ideal Hubble diagram with no dispersion, and in the upper right panel we have added the dispersion owing to lensing ("lens") in a universe with 20% compact objects and 80% smooth DM halos parametrized by the NFW formula. Comparing this with the panel in the lower left, where the intrinsic dispersion ("intr") and measurement error ("err") have been included, we see that the effects become comparable at a redshift of unity. In the lower right panel we see the most realistic simulation with intrinsic dispersion, measurement error, and lensing dispersion.

Of course, the additional dispersion caused by gravitational lensing will be a source of systematic error in the cosmological parameter determination with SNe Ia. However, a possible virtue of lensing is that the distribution of luminosities might be used to obtain some information on the matter distribution in the universe, e.g., to determine the fraction of compact DM in our universe.

4. SUPERNOVA OBSERVATION CALCULATOR

To perform realistic calculations we have developed a numerical simulation package, the supernova observation calculator (SNOC). It can be used to estimate various systematic effects such as dust extinction and gravitational lensing on current SN measurements as well as the accuracy to which various parameters can be measured with future SN searches. In this paper, we use SNOC to obtain simulated samples of the intrinsic dispersion and gravitational lensing effects of SNe Ia over a broad redshift range.

The intrinsic dispersion and measurement error is represented by a Gaussian distribution with $\sigma_m = 0.16$ mag. Gravitational lensing effects are calculated by tracing the light between the source and the observer by sending it through a series of spherical cells in which the DM distribution can be specified. (For more details on the method originally proposed by Holz and Wald, see Holz & Wald 1998 and Bergström et al. 2000.)

We will model compact DM as point masses and smooth DM as the NFW density profile. The exact parameterization of the smooth DM halo profile is not important for the results obtained in this paper (Bergström et al. 2000). The results are also independent of the individual masses of the compact objects as well as their clustering properties on galaxy scales (Holz & Wald 1998; Bergström et al. 2000). As we have seen, the eventual small-scale structure in the "smooth" component does not act as a compact component.

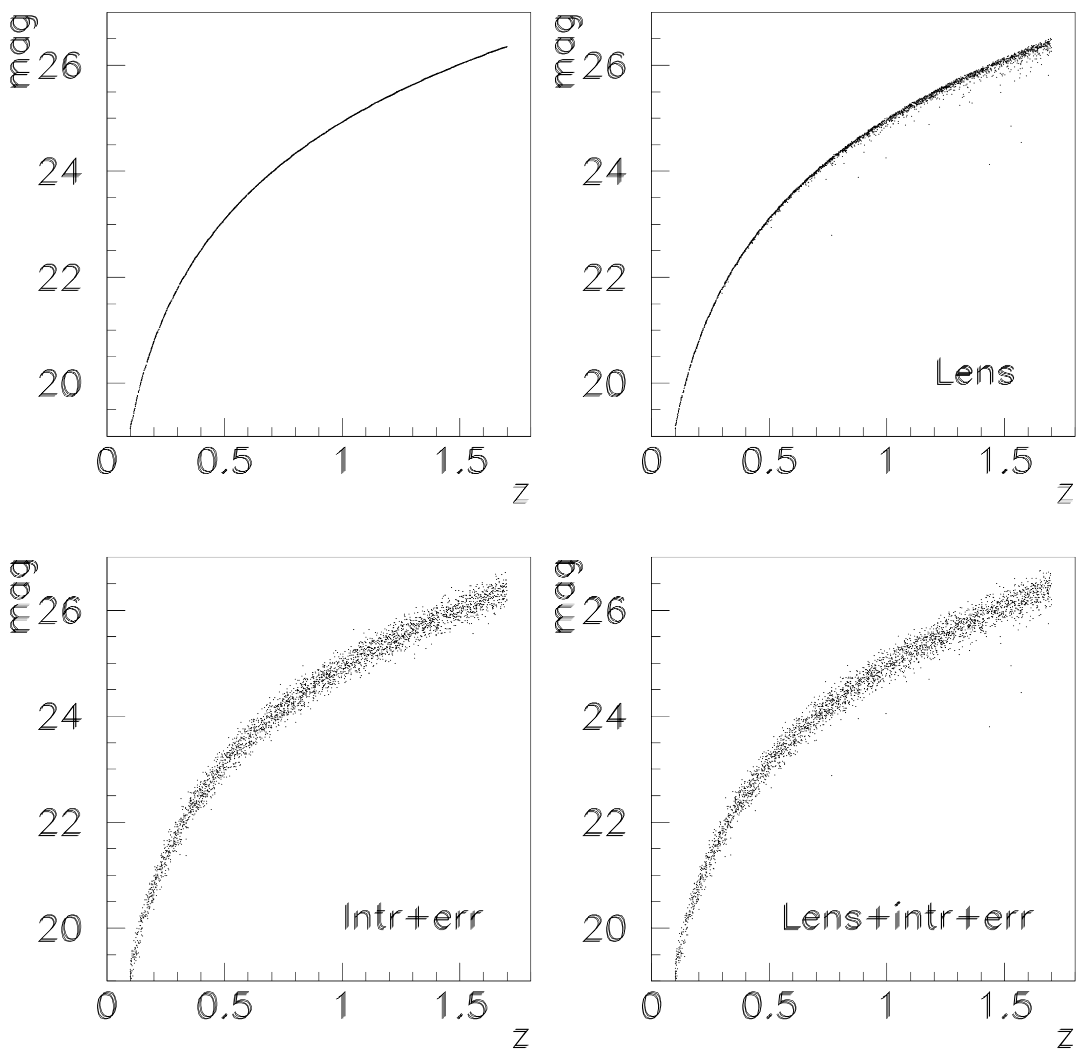

FIG. 1.—Comparison of the dispersion owing to lensing (*upper right panel*) and the measurement error and intrinsic dispersion of SNe Ia (*lower left panel*).

5. *SUPERNOVA/ACCELERATION PROBE*

To make realistic predictions of the statistics and quality of the supernova sample, we use the projected discovery potential of the *SNAP* project. This is a proposed satellite telescope capable of discovering over 2000 SNe Ia per year in the redshift range $0.1 < z < 1.7$ (see footnote 2). The most anticipated use of the data is to gain further accuracy in the determination of, e.g., Ω_M and the curvature of the universe Ω_k but also to give insight into the nature of the negative pressure energy component by constraining the equation of state (Huterer & Turner 1999; Goliath et al. 2001) or the redshift dependence of the effective energy density (Tegmark 2001). Here we show how the data can also be used to give information on the fraction of compact objects in the DM component.

More specifically, it is projected that in 1 yr, *SNAP* will be able to discover, follow the light curves, and obtain spectra for on the order of 2000 SNe. While the exact redshift distribution of the SNe Ia to be followed by *SNAP* might be changed upon studies of the optimal search strategies for the primary goals of the project, we have used the Monte Carlo–generated sample spectra of 2366 SNe distributed according to the *SNAP* Proposal (see footnote 2). (See Fig. 2 to make specific predictions.)

6. RESULTS

Using SNOC, we have created large data sets of synthetic SNe observations with a variable fraction of compact objects ranging from 0% to 40% using the following cosmo-

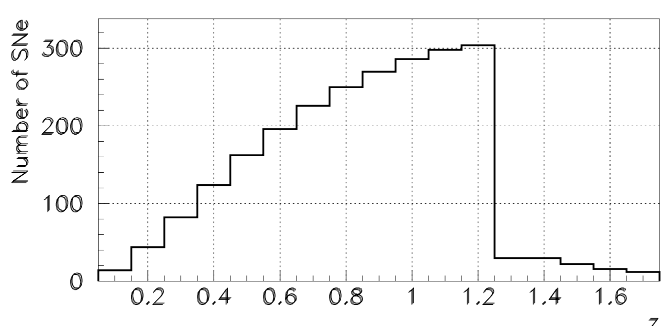

FIG. 2.—Number of SNe Ia expected for various redshift bins in a 1 yr exposure with the proposed *SNAP* satellite. The data are taken from Table 7.2 in the *SNAP* Proposal (see footnote 2).

logical background parameter values: $\Omega_M = 0.3$, $\Omega_\Lambda = 0.7$, and $h = 0.65$. (For a discussion of how the halo distributions were generated, see Bergström et al. 2000.) These data sets are used as reference samples.

In Figures 3 and 4, we have plotted the dispersion in the reference samples for 0% (*solid line*), 20% (*dashed line*), and 40% (*dotted line*) compact objects in logarithmic and linear scale, respectively. In the upper panels, the lensing dispersion is plotted; i.e., the dashed line basically corresponds to the scatter in the upper right panel in Figure 1. The zero-value corresponds to the value one would obtain in a homogeneous universe (Fig. 1, *upper left panel*). Note that negative values correspond to magnified events, positive values to demagnified events. As the fraction of compact DM grows, lensing effects become larger in the sense that we get a broader distribution of magnifications. From Figure 3, it is clear how the high-magnification tail grows with the fraction in compact objects. In Figure 4, we see that there is also a shift in the peak of the distribution. In the lower panel we have added a Gaussian intrinsic dispersion and measurement error, $\sigma_m = 0.16$ mag, making the distributions look more similar (cf. Fig. 1, *lower right panel*). Although this smearing obviously decreases the significance of the compact signal, it can be seen that the high-magnification tails and the shifts in the peak of the distributions are still visible.

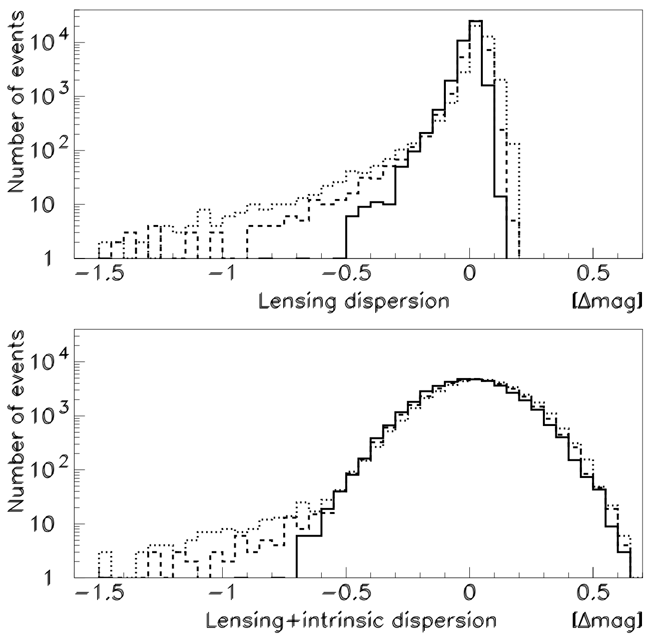

FIG. 3.—Magnitude dispersion of reference samples for 0% (*solid line*), 20% (*dashed line*), and 40% (*dotted line*) compact objects using logarithmic scale. The bottom panel includes a Gaussian smearing, $\sigma_m = 0.16$ mag, owing to intrinsic brightness differences between supernovae and from measurement error. The distributions show the projected scatter around the ideal Hubble diagram for SNe Ia with a relative redshift distribution as in Fig. 2.

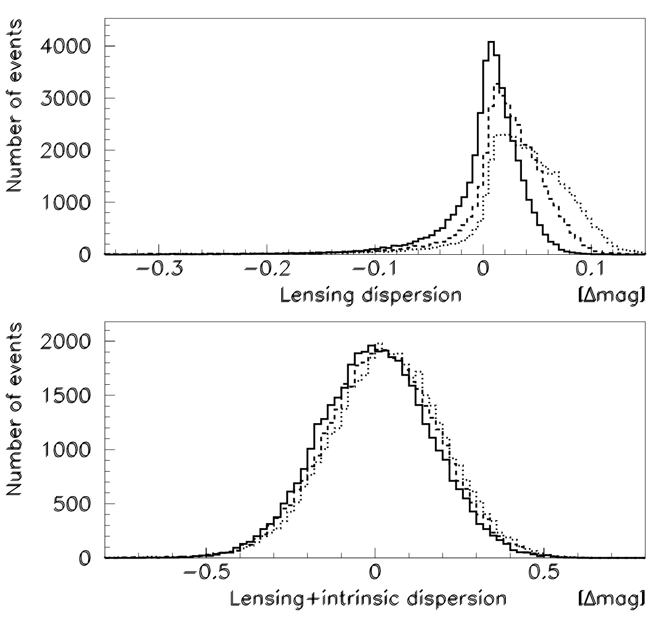

FIG. 4.—Magnitude dispersion of reference samples for 0% (*solid line*), 20% (*dashed line*), and 40% (*dotted line*) compact objects using linear scale (cf. Fig. 3). The bottom panel includes a Gaussian smearing, $\sigma_m = 0.16$ mag.

We have also created a large number of simulated 1 yr *SNAP* data sets (according to Fig. 2 above) with 6%, 11%, and 21% compact objects. These are our experimental samples. By comparing each generated experimental sample with our high-statistics reference samples using the Kolmogorov-Smirnov (K-S) test, we obtain a confidence level for the hypothesis that the experimental sample is drawn from the same distribution as the reference sample. For each fraction of compact objects in the experiments (6%, 11%, and 21%), we repeat this procedure for 1000 experimental realizations and pick out the reference sample that gives the highest confidence level for each experiment. Plotting the number of best-fit reference samples as a function of the fraction of compact objects in the reference sample, we can fit a Gaussian and thus estimate the true value and the dispersion. In each case, we get a mean value within 1% of the true value and a 1 σ error less than 5% (see Fig. 5).

As one could expect, and is shown in Figure 1, lensing effects get larger at higher redshifts. At low redshifts the dispersion is completely dominated by the intrinsic dispersion. Therefore, we have used only the data from SNe at $z > 0.8$, a total of 1387 SNe, to obtain the result in Figure 5. Of course, the data from SNe at $z < 0.8$ can still be used to constrain the values of Ω_M and Ω_Λ. In fact, with 1 yr of *SNAP* data, it is possible to determine Ω_M with a statistical uncertainty of $\Delta\Omega_M \approx 0.02$ (see footnote 2).

Since it is not clear whether the discrimination of samples is most sensitive to changes in the high-magnification tail or to shifts in the peak of the distributions, we have performed a number of statistical tests besides the K-S test, which is most sensitive to differences at the peak of the distributions. These tests includes variants on the K-S test designed to increase the sensitivity in the tails of the distributions (Anderson-Darling, Kuiper, etc.) as well as a maximum likelihood analysis. We have found that the K-S test gives the most robust results for our purposes.

In the analysis so far, we have assumed that Ω_M and Ω_Λ will be known to an accuracy where the error in luminosity is negligible in comparison to the intrinsic and lensing dispersion of SNe Ia. This assumption is not unreasonable with future CMBR observations combined with other cosmological tests and the *SNAP* data itself, nor is it crucial in the sense that we are dealing with the dispersion of luminosities around the true mean value, not the mean value itself. In order to test the sensitivity of our results to changes

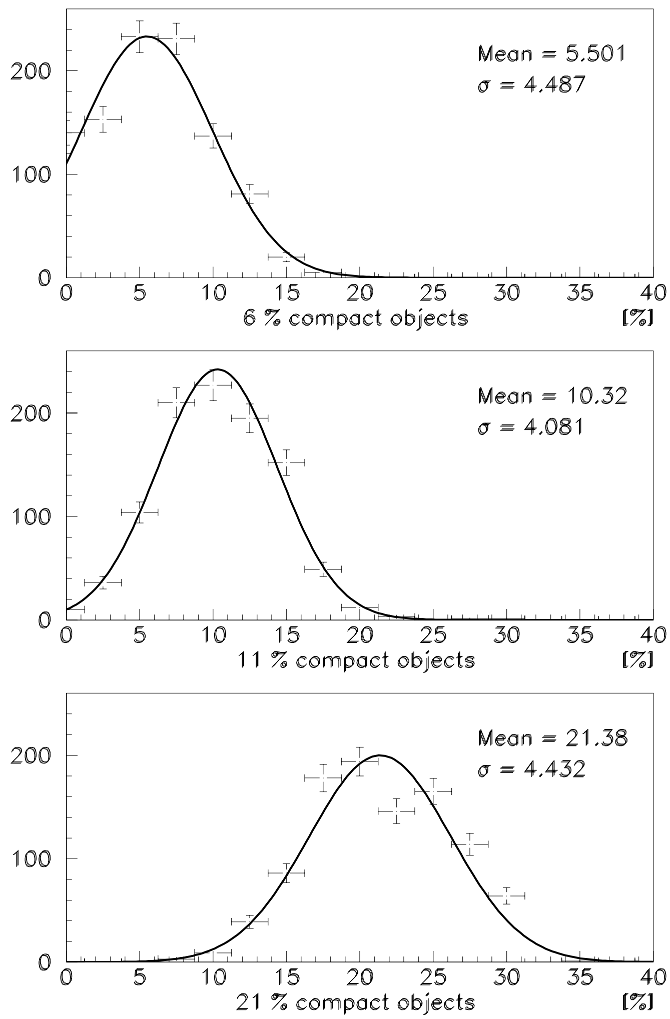

FIG. 5.—Number of best-fit reference samples as a function of the fraction of compact objects in the reference sample.

in the cosmological parameter values, we have performed a number of Monte Carlo simulations using different sets of parameters in our experimental and reference samples and found the error in the total energy density in compact objects to be negligible. Note that the effect from lensing is proportional to the total energy density in compact objects, not the fraction of compact objects (see, e.g., Schneider, Ehlers, & Falco 1992). A higher Ω_M would therefore increase the sensitivity for smaller fractions. Also, we have used a value of the intrinsic dispersion and measurement error of $\sigma_m = 0.16$ mag, a value that may be appreciably smaller in the future when the large data sample expected may allow, e.g., a more refined description and classification of supernovae. Using simulated data sets with $\sigma_m = 0.1$ mag, the 1 σ error in the determination of the fraction of compact objects using the same cosmology as above becomes less than 3%, as depicted in Figure 6.

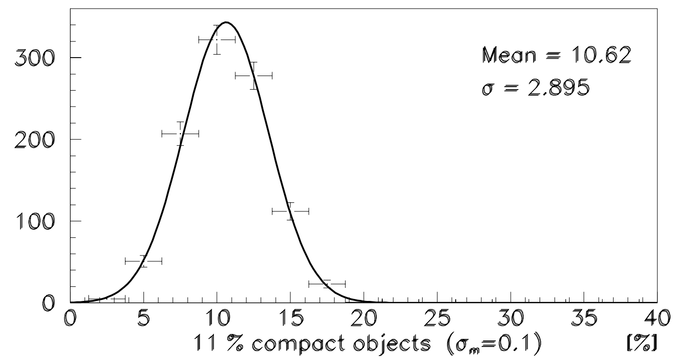

FIG. 6.—Number of best-fit reference samples as a function of the fraction of compact objects in the reference sample for an intrinsic dispersion and measurement error of $\sigma_m = 0.1$ mag.

The virtues of the method we use in this paper is that since Monte Carlo methods are used to generate our samples as well as to analyze the data, we do not need to parametrize the probability density functions (PDFs) for different fractions of compact objects. Also, since we use the K-S test, we do not have to bin our data in order to perform our statistical analysis. A possible drawback is that we do not include the effects from large-scale structures in our lensing calculations as done in Seljak & Holz (1999). However, since our modeling of the structure is very detailed up to galaxy scales (see Goliath & Mörtsell 2000), the two approaches should be complementary to each other. Of course, it should be possible to combine the PDFs from large-scale structures with the PDFs from galaxy scales that we obtain from our Monte Carlo simulations, but we have not yet performed such an analysis.

7. SUMMARY

The proposed *SNAP* satellite will be able to detect and obtain spectra for more than 2000 SNe Ia per year. In this paper we have used simulated data sets obtained with the SNOC simulation package to show how 1 yr of *SNAP* data can be used to determine the fraction of compact DM in our universe to $\lesssim 5\%$ accuracy, assuming the intrinsic dispersion and measurement error is $\sigma_m = 0.16$ mag. If the intrinsic dispersion and measurement error can be further reduced, e.g., from a improved understanding of SN Ia detonation mechanisms, the accuracy can be improved even further.

The authors would like to thank Uros Seljak for helpful comments improving the quality of the manuscript. L. B. wishes to thank the Swedish Research Council for financial support and the Institute for Advanced Study at Princeton for hospitality when part of this work was performed. A. G. is a Royal Swedish Academy Research Fellow supported by a grant from the Knut and Alice Wallenberg Foundation.

REFERENCES

Alcock, C., et al. 2000, ApJ, 542, 281
Bahcall, N. A., & Fan, X. 1998, ApJ, 504, 1
Bergström, L., Goliath, M., Goobar, A., & Mörtsell, E. 2000, A&A, 358, 13
Burles, S., Nollett, K. M., Truran, J. N., & Turner, M. S. 1999, Phys. Rev. Lett., 82, 4176
Carlberg, R. G., Yee, H. K. C., Morris, S. L., Lin, H., Ellingson, E., Patton, D., Sawicki, M., & Shepherd, C. W. 1999, ApJ, 516, 552
Fukugita, M., Hogan, C. J., & Peebles, P. J. E. 1998, ApJ, 503, 518
Ghigna, S., Moore, B., Governato, F., Lake, G., Quinn, T., & Stadel, J. 2000, ApJ, 544, 616
Goliath, M., Amanullah, R., Astier, P., Goobar, A., & Pain, R. 2001, preprint (astro-ph 0104009)
Goliath, M., & Mörtsell, E. 2000, Phys. Lett. B, 486, 249
Holz, D. E., & Wald, R. M. 1998, Phys. Rev. D, 58, 063501
Huterer, D., & Turner, M. S. 1999, Phys. Rev. D, 60, 081301
Jedamzik, K. 1998, Phys. Rev. D, 55, 5871

Lasserre, T., et al. 2000, A&A, 355, L39
Metcalf, R. B., & Silk, J. 1999, ApJ, 519, L1
Navarro, J. F., Frenk, C. S., & White, S. D. M. 1997, ApJ, 490, 493
Netterfield, C. B., et al. 2001, preprint (astro-ph/0104460)
Peacock, J. A., et al. 2001, Nature, 410, 169
Perlmutter, S., et al. 1999, ApJ, 517, 565
Persic, M., & Salucci, P. 1992, MNRAS, 258, 14
Pryke, C., et al. 2001, preprint (astro-ph/0104490)
Rauch, K. P. 1991, ApJ, 374, 83
Riess, A. G., et al. 1998, AJ, 116, 1009
Schneider, P., Ehlers, J., & Falco, E. E. 1992, Gravitational Lenses (Berlin: Springer)
Seljak, U., & Holz, D. 1999, A&A, 351, L10
Stompor, R., et al. 2001, preprint (astro-ph/0105062)
Tegmark, M. 2001, preprint (astro-ph/0101354)
Wang, X., Tegmark, M., & Zaldarriaga, M. 2001, preprint (astro-ph/0105091)